

Article

Land Cover Change Prediction Modeling in Tanjungpinang City in 2043

Article Info

Article history :

Received June 12, 2025

Revised June 17 2025

Accepted June 20, 2025

Published September 30, 2025

In Press

Keywords :

Land cover, prediction,
remote sensing,
logistic regression

Arie Afriadi^{1*}, Nefriwati Hilmi¹, Hoki Apriyenson¹,
Zuleriwati AS¹

¹Department of Urban and Regional Planning, Faculty of Engineering and Marine Technology, Universitas Maritim Raja Ali Haji, Tanjungpinang, Indonesia

Abstract. Land cover changes reflect the pressure of development and increased human activities that have an impact on environmental imbalance. As a strategic coastal city, Tanjungpinang faces challenges in maintaining the sustainability of its regional ecosystem. This study aims to analyze the dynamics of land cover changes and predict their conditions until 2043 using remote sensing technology and geographic information systems (GIS), incorporating Cellular Automata and logistic regression methods. The results of the study showed that land cover changes between 2003 and 2023 increased built-up area by 27.15 km² and decreased Vegetation by 14.02 km². Bare Land increased by 1.45 km² at the beginning of the period, then reduced to a total of 12.74 km². Water bodies decreased by 0.39 km². Predictions for 2043 indicate that built-up area increased by 5.12 square kilometres, while Vegetation decreased by 6.33 square kilometres. Bare land increased by 1.34 km², while water bodies declined by 0.14 km². This pattern indicates a trend of converting vegetative land into built-up areas due to the increasing demand for regional space.

This is an open-access article under the [CC-BY](#) license.



This is an open-access article distributed under the Creative Commons 4.0 Attribution License, which permits unrestricted use, distribution, and reproduction in any medium, provided the original work is properly cited. ©2025 by the author.

Corresponding Author :

Arie Afriadi

Department of Urban and Regional Planning, Faculty of Engineering and Maritime Technology
Universitas Maritim Raja Ali Haji, Tanjungpinang, Indonesia

Email : arieafriadi@umrah.ac.id

1. Introduction

Land cover changes in various regions are the result of complex interactions between human activities and natural systems, where urbanization, land conversion, and infrastructure development are the main factors driving this transformation [1]. Population growth and rapid economic growth have created tremendous pressure on land availability, while the need for space for settlements, industrial areas, and infrastructure continues to increase in the face of limited available land, thus encouraging land conversion from natural conditions to built-up regions [2]. The impact of this change is not only seen in the physical transformation of the surface but also disrupts the balance of the ecosystem by affecting water flow patterns and microclimate conditions and causing various environmental problems such as increased surface runoff, decreased soil absorption capacity, and disruption of the sustainability of natural habitats [3].

Tanjungpinang City, as the capital of the Riau Islands Province, has experienced rapid development over the last few decades, marked by an increase in population and a growing need for housing, infrastructure, and supporting facilities such as transportation, trade centres, and public spaces [4]. However, the progress of a city does not always have a uniformly positive impact. Behind the physical and economic growth, various adverse environmental impacts have emerged [5]. One of the most significant impacts is the massive conversion of land use, especially the conversion of green open spaces into built-up areas [6]. This condition results in a decline in environmental quality marked by a reduction in air catchment areas, an increased risk of accumulation and flooding, and an increase in surface temperatures due to the effects of urban heat. Rapid changes in land cover without sacrificing effective spatial control also trigger conflicts over the use of space, ecosystem degradation, and the loss of the city's ecological function. The similarity between physical development and environmental preservation reflects the weak integration of poverty principles in city planning [7]. As a coastal city that has a strategic role in supporting regional growth, Tanjungpinang faces serious challenges related to the dynamics of land cover changes [8]. These changes not only impact local environmental conditions but also affect environmental dynamics at the regional level. Therefore, a comprehensive understanding of land cover change trends is required, including pattern analysis and predictions of future changes as a basis for making appropriate decisions in preparing sustainable spatial plans [9].

Studies on land use changes in Tanjungpinang City have been conducted in previous studies, such as the study [10], which focuses on the development of residential areas and land use predictions using the Land Change Modeler (LCM) based on secondary data in the form of land use maps. Unlike previous studies, this study utilizes primary data in the form of Landsat satellite imagery, interpreted using the Maximum Likelihood Classification (MLC) method, to produce a multitemporal land cover map. This approach provides a more accurate and objective representation of the spatial conditions of the area. Furthermore, this study integrates the Cellular Automata (CA) method and logistic regression to model land cover changes spatially and temporally until 2043, which aligns with the planning period in the Tanjungpinang City RTRW 2024–2044.

This study aims to analyze land cover changes and predict future land cover conditions in Tanjungpinang City by utilizing remote sensing technology and Geographic Information Systems (GIS) [11]. The combination of the two technologies provides a strong ability to analyze the dynamics of land cover changes, considering various factors that influence them [12]. The driving factors considered in this study include road networks, built-up areas, slope gradients, elevations, rivers, and population density. All of these factors play an important role in explaining land change patterns and are used as variables in predicting land cover conditions in Tanjungpinang City in 2043 [13]. For simulation and prediction purposes, the cellular automata (CA) method is used, which is known to be accurate in modelling spatial and temporal changes in the land [14]. This model has the advantage of producing accurate and dynamic spatial-temporal predictions and can effectively describe complex spatial phenomena. Additionally, the logistic regression method is employed to elucidate the

relationship between the dependent variable, represented by the land cover category, and the independent variables at both interval and categorical scales [15]. Analysis was conducted on Landsat satellite imagery data from 2003, 2013, and 2023 as a basis for predicting land cover conditions in 2043.

The research location is in Tanjungpinang City, Riau Islands, situated on the coast of Bintan Island. The city is located at coordinates $0^{\circ}55'00''\text{N} - 1^{\circ}10'00''\text{N}$ and $104^{\circ}23'00''\text{E} - 104^{\circ}35'00''\text{E}$. Geographically, the boundaries of Tanjungpinang City include the Natuna Sea to the north, Bintan Regency to the east and west, and the Natuna Sea and Bintan Regency to the south. Tanjungpinang City has an area of approximately 150 km^2 , consisting of four sub-districts [16].

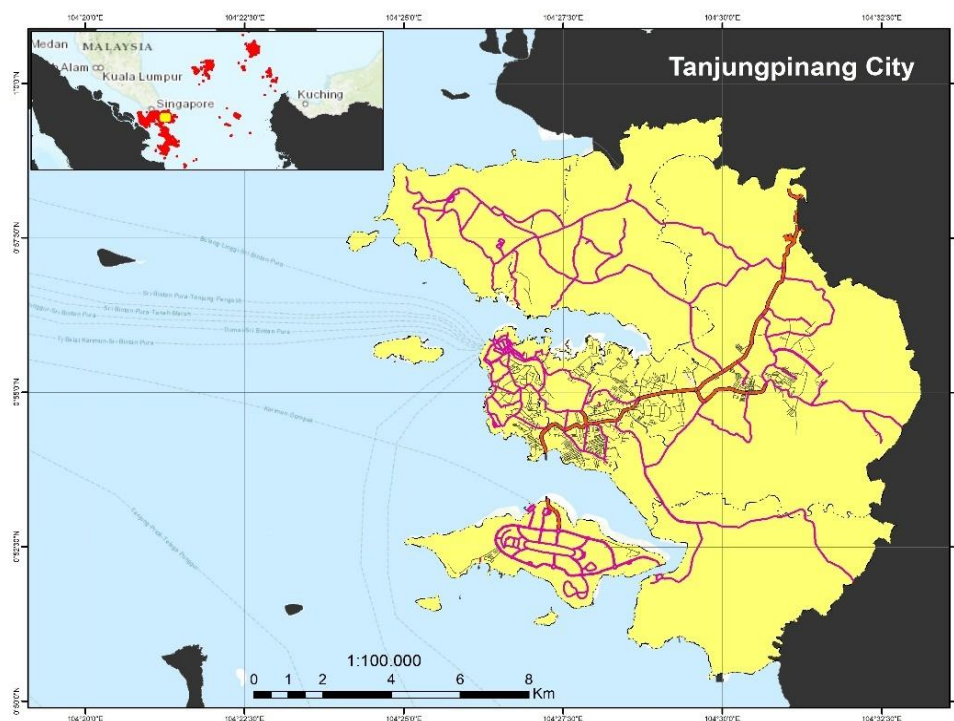


Figure 1. Research area

2. Materials and Methods

This study utilizes several software tools to support the analysis and prediction of land cover changes through 2043. ArcGIS 10.8 and QGIS 3.34, along with the MOLUSCE (Modules for Land Use Change Evaluation) plugin, are utilized for spatial analysis and modelling land cover change. Microsoft Office 2019 is used in document processing and reporting. Additionally, Google Earth Engine (GEE) is utilized as a cloud-based platform for processing and analyzing satellite imagery data, supported by the JavaScript programming language, which is run online through the official Google Earth Engine page (<https://earthengine.google.com/>).

The primary data in this study consists of Landsat 5 TM satellite imagery (2003) and Landsat 8 OLI (2013 and 2023), which are used to identify land cover changes based on the observation period. Other supporting data include the Tanjungpinang City administrative map, the Indonesian Topographic Map (RBI), the National Digital Elevation Model (Demnas), road networks, river networks, and population data. All of these data serve as input in spatial analysis and land cover prediction modelling.

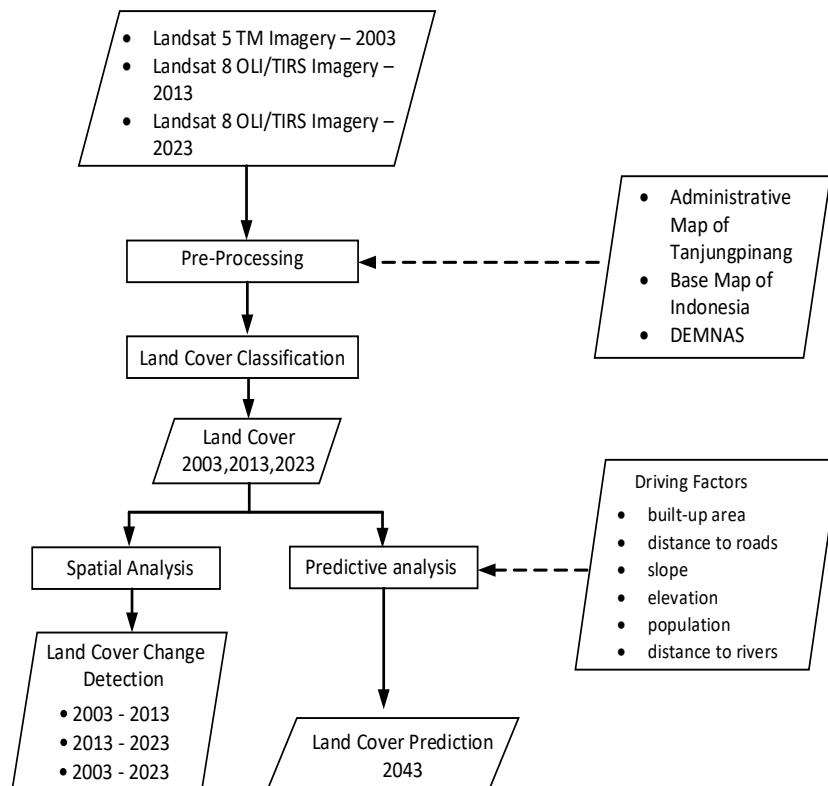


Figure 2. Framework diagram

2.1 Pre-Processing

The pre-processing stage is the initial step in processing Landsat satellite imagery before the primary analysis is carried out [17]. At this stage, radiometric correction is applied to improve the visual quality and accuracy of pixel spectral values. Furthermore, a cropping process is performed on the Landsat image to align with the boundaries of the research area.

2.1.1 Radiometric Correction

Radiometric correction in this study was performed using the Google Earth Engine (GEE) platform [18]. This correction process was applied to Landsat 5 Thematic Mapper (TM) and Landsat 8 Operational Land Imager (OLI) images, which are the primary sources of remote sensing data in the study. Correction was carried out until it reached the Top of Atmosphere (TOA) reflectance stage, which is the stage of converting Digital Number (DN) values into reflectance values that describe the amount of reflected energy above the atmosphere. This step is crucial for enhancing the accuracy of spectral values, minimizing the impact of atmospheric disturbances, and ensuring that the data used has sufficient consistency and quality before proceeding with further analysis.

2.1.2 Composite Band

After Landsat 5 and Landsat 8 image data undergo radiometric correction to reach the Top of the Atmosphere (TOA) stage, a multispectral band merging process (composite band) is carried out [19]. This process aims to integrate information from each spectral channel into a single composite image that represents the characteristics of the Earth's surface objects more comprehensively, as well as to facilitate identification and interpretation. For Landsat 5-TM imagery, the composite is created using Bands 1 (blue), 2 (green), 3 (red), 4 (near-infrared), 5 (shortwave infrared 1), and 7 (shortwave infrared

2). Meanwhile, in Landsat 8-OLI imagery, Bands 1 (coastal), 2 (blue), 3 (green), 4 (red), 5 (near-infrared), 6 (shortwave infrared 1), and 7 (shortwave infrared 2) are used.

2.1.3 Clip/Cropping

After the multispectral band merging process is complete, the next stage is to crop or cut the image. Cropping is done to limit the coverage area of satellite imagery to only the areas that are the focus of the research [20]. This step is used for data processing efficiency and to focus the analysis on relevant areas. The cropping process is carried out on Landsat 5-TM and Landsat 8-OLI images. Cropping is done based on the administrative boundaries of Tanjungpinang City.

2.2 Land Cover Classification

The land cover classification used in this study refers to the approach proposed by [26], which divides land cover into four main classes, namely water bodies, built-up land, Vegetation, and bare land. In this classification, each land cover class encompasses several types of land use that share similar physical characteristics and functions, as outlined in Table 1. These classifications are designed to simplify the analysis of satellite imagery by grouping similar land use types into broader, more manageable categories. For instance, the vegetation class may encompass forests, plantations, and grasslands, all characterized by the presence of dense or sparse vegetation cover. Built-up land encompasses residential areas, commercial zones, and infrastructure, including roads and buildings, reflecting human-altered landscapes. Water bodies comprise rivers, lakes, and coastal waters, while bare land typically refers to exposed soil, rocky surfaces, or areas with minimal Vegetation. This standardized classification enhances the consistency and comparability of land cover change analysis over time and across different regions.

Table 1. Land cover classification

Land Cover	Description
Water Body	Rivers, wetlands, lakes, ponds and reservoirs
Bare Land	Vacant lands, open areas, sandy surfaces, and landfill or waste disposal areas
Built-up Area	Residential developments, commercial and industrial areas, and transportation infrastructure
Vegetation	Urban parks, tree cover, grasslands, and agricultural areas

Land cover classification is done using the Supervised Classification approach. Supervised classification is a digital image processing method that identifies and categorizes pixels into specific classes based on their spectral characteristics [21] [22]. One commonly used approach is Maximum Likelihood Classification (MLC), which assumes that the spectral distribution of each class follows a pattern. This method determines pixel membership in a class based on the highest probability by utilizing statistical estimates, including mean vectors and covariance matrices, derived from training samples. The representativeness of the training data significantly influences the success of the classification, as inaccurate estimates can lead to less accurate classifications [23].

Land cover classification using the supervised classification method is carried out by manually determining the training area through visual interpretation of composite Landsat imagery, taking into account topographic map information [21]. The user selects representative areas for each land cover class, such as built-up areas, water bodies, Vegetation, and Bare land. From these areas, several pixels are selected as training samples based on the similarity of hue, colour, and texture [24]. These samples are then analyzed using the image to obtain the statistical information needed for the classification process. To ensure consistency and accuracy of the results, the training area is selected from an area with a high level of homogeneity [25].

2.3 Land Cover Change Analysis

Land Cover Change Analysis Using Overlay Techniques. Overlay techniques are a method in spatial analysis used to combine multiple layers of spatial data with the same geographic reference to produce new information. In the context of Geographic Information Systems (GIS), overlay techniques are used to identify spatial changes that occur over time in a systematic and structured manner [27].

In this study, the overlay technique was used to map land cover changes in two time periods, namely 2003–2013, 2013–2023, and 2003–2023. The overlay process was conducted in pairs for each period to identify spatial changes within each land cover class. Through this stage, information was obtained regarding land cover dynamics, which revealed shifts in land use classes over a specific period.

2.4 Land Cover Prediction Analysis

The selection of the Cellular Automata (CA) method, combined with logistic regression, in this study, is based on the data characteristics and analysis objectives that require a spatial-temporal predictive approach. With a long period of land cover observation, spanning 2003, 2013, and 2023, a method is needed that can capture patterns of change that occur gradually over the medium to long term. Logistic regression is used to identify and measure the influence of driving factors on land cover change. The results of this regression are in the form of change probabilities, which serve as the basis for modelling using Cellular Automata. CA functions to project changes dynamically by considering spatial proximity between cells. The combination of these two methods accurately captures the complexity of land changes over a long period of time. In the application, the Cellular Automata (CA) and Logistic Regression (LR) models are processed through the MOLUSCE plugin in QGIS 3.34 software [15, 28]. The CA model functions to represent the dynamics of land cover change in a geospatial context. At the same time, the LR method is used to identify statistical relationships between land cover and various driving factors, such as distance to roads, distance to rivers, population density, elevation, slope, and proximity to built-up areas.

The prediction stage begins by using land cover data from 2003 and 2013 as a basis for modelling land cover projections for 2023. The prediction results are then validated for accuracy by comparing them to actual data from 2023, which measures the level of model accuracy based on the Kappa value. After validation shows acceptable results, the model will continue to project land cover changes until 2043. The Kappa statistical test is used to evaluate the level of classification accuracy based on the error matrix. The Kappa coefficient value ranges from 0 to 1, is generally lower than the overall accuracy value, and can be calculated using the following formula [29]:

$$\text{Kappa accuracy} = \frac{N \sum_{i=1}^r x_{ii} - \sum_{i=1}^r (x_{i+} x_{+i})}{N^2 - \sum_{i=1}^r (x_{i+} x_{+i})}$$

The letter r indicates the number of rows in the matrix, x_{ii} is the number of observations in the i-th row and i-th column, while x_{i+} and x_{+i} represent the total margin for the i-th row and i-th column, respectively. N refers to the total number of all observations. Model validation plays a crucial role in assessing the accuracy of prediction results [30]. The Kappa accuracy level falls within the range of values between 0 and 1 [29], as shown in Table 2.

Table 2. Kappa value

Kappa Value	Classification
< 0.20	Poor
0.21 – 0.40	Fair
0.41 – 0.60	Moderate
0.60 – 0.80	Good
0.81 – 1.00	Very Good

After the model shows an acceptable level of accuracy, the process continues by projecting land cover changes until 2043. In this study, the time interval from 2003 to 2013 spans 10 years, so one iteration in the model represents this period. Therefore, the land cover projection for 2043 is carried out through two consecutive iterations, namely from 2013 to 2023 (first iteration) and from 2023 to 2043 (second iteration). All stages of prediction and this iteration process are carried out using the MOLUSCE plugin in QGIS software [31].

3. Results and Discussion

3.1 Pre-Processing

Landsat image pre-processing was carried out using the Google Earth Engine (GEE) platform with stages arranged to support land cover analysis. The steps taken include determining the study area (Region of Interest/ROI), selecting images based on their IDs, converting them to Top of Atmosphere (TOA) reflectance, compiling band composites, and exporting the processed images. This entire process was applied consistently to data from 2003, 2013, and 2023, ensuring that the results of the spatial analysis can be compared fairly and objectively. Figure 3 shows the script used in this process.

2003	2013	2023
<pre> 1 // Mendefinisikan ROI (Polygon) yang digunakan 2 var ROI = ee.Geometry.Polygon([3 [4 [104.36879374934832, 0.8242373465188328], 5 [104.56404881566882, 0.8242373465188328], 6 [104.56404881566882, 0.9986231718896573], 7 [104.36879374934832, 0.9986231718896573], 8 [104.36879374934832, 0.8242373465188328] 9] 10]); 11 12 // Mendapatkan citra Landsat 5 (TM) untuk tahun 2000-2001 13 var dataset = ee.ImageCollection('LANDSAT/LT05/C02/T1') 14 .filterBounds(ROI) 15 .filterDate('2003-01-01', '2003-12-31'); 16 17 print(dataset); 18 19 // Memilih citra spesifik berdasarkan ID 20 var single = ee.Image('LANDSAT/LT05/C02/T1/LT05_125859_20030319'); 21 var potong = single.clip(ROI); 22 23 // Menghitung TOA (Top of Atmosphere) 24 var TOA = ee.Algorithms.Landsat.TOA(potong); 25 26 // Komposit True Color 27 var trueColor = TOA.select(['B3', 'B2', 'B1']); 28 Map.addLayer(trueColor, {min: 0, max: 0.3}, 'True Color (Landsat 5)'); 29 30 // Komposit Band B1, B2, B3, B4, B5, B7 31 var compositeBand = TOA.select(['B1', 'B2', 'B3', 'B4', 'B5', 'B7']); 32 Map.addLayer(compositeBand, {min: 0, max: 0.3}, 'Composite Band 1-2-3-4-5-7'); 33 34 // Ekspor komposit 6 band ke Google Drive 35 Export.image.toDrive({ 36 image: compositeBand, 37 description: 'Landsat5_Composite_B1_B7', 38 scale: 30, 39 region: ROI, 40 fileFormat: 'GeoTIFF', 41 maxPixels: 1e8 42 }); 43 </pre>	<pre> 1 // Mendefinisikan ROI (Polygon) yang digunakan 2 var ROI = ee.Geometry.Polygon([3 [4 [104.36879374934832, 0.8242373465188328], 5 [104.56404881566882, 0.8242373465188328], 6 [104.56404881566882, 0.9986231718896573], 7 [104.36879374934832, 0.9986231718896573], 8 [104.36879374934832, 0.8242373465188328] 9] 10]); 11 12 // Mendapatkan citra Landsat 8 (OLI/TIRS) untuk tahun 2012-2013 13 var dataset = ee.ImageCollection('LANDSAT/LC08/C02/T1') 14 .filterBounds(ROI) 15 .filterDate('2013-01-01', '2013-12-31'); 16 17 print(dataset); 18 19 // Memilih citra spesifik berdasarkan ID 20 var single = ee.Image('LANDSAT/LC08/C02/T1/LC08_125859_20130627'); 21 print(single, 'Selected Image'); 22 23 var potong = single.clip(ROI); 24 25 // Menghitung TOA (Top of Atmosphere) 26 var TOA = ee.Algorithms.Landsat.TOA(potong); 27 28 // Komposit True Color 29 var trueColor = TOA.select(['B4', 'B3', 'B2']); 30 Map.addLayer(trueColor, {min: 0, max: 0.3}, 'True Color (Landsat 8)'); 31 32 // Komposit Band B1-B7 dan B9 33 var compositeBand = TOA.select(['B1', 'B2', 'B3', 'B4', 'B5', 'B6', 'B7', 'B9']); 34 Map.addLayer(compositeBand, {min: 0, max: 0.3}, 'Composite Band 1-2-3-4-5-6-7-9'); 35 36 // Ekspor komposit 8 band ke Google Drive 37 Export.image.toDrive({ 38 image: compositeBand, 39 description: 'Landsat8_Composite_B1_B7_B9', 40 scale: 30, 41 region: ROI, 42 fileFormat: 'GeoTIFF', 43 maxPixels: 1e8 44 }); 45 </pre>	<pre> 1 // Mendefinisikan ROI (Polygon) yang digunakan 2 var ROI = ee.Geometry.Polygon([3 [4 [104.36879374934832, 0.8242373465188328], 5 [104.56404881566882, 0.8242373465188328], 6 [104.56404881566882, 0.9986231718896573], 7 [104.36879374934832, 0.9986231718896573], 8 [104.36879374934832, 0.8242373465188328] 9] 10]); 11 12 // Mendapatkan citra Landsat 8 (OLI/TIRS) untuk tahun 2022-2023 13 var dataset = ee.ImageCollection('LANDSAT/LC08/C02/T1') 14 .filterBounds(ROI) 15 .filterDate('2023-01-01', '2023-12-31'); 16 17 print(dataset, 'Dataset'); 18 19 // Memilih citra spesifik berdasarkan ID 20 var single = ee.Image('LANDSAT/LC08/C02/T1/LC08_125859_20230725'); 21 print(single, 'Selected Image'); 22 23 var potong = single.clip(ROI); // Menotong citra dengan ROI 24 25 // Menghitung TOA (Top of Atmosphere) 26 var TOA = ee.Algorithms.Landsat.TOA(potong); 27 28 // Komposit True Color (RGB) 29 var trueColor = TOA.select(['B4', 'B3', 'B2']); 30 Map.addLayer(trueColor, {min: 0, max: 0.3}, 'True Color (Landsat 8)'); 31 32 // Komposit B1-B7 dan B9 33 var compositeB79 = TOA.select(['B1', 'B2', 'B3', 'B4', 'B5', 'B6', 'B7', 'B9']); 34 Map.addLayer(compositeB79, {min: 0, max: 0.3}, 'Composite B1-B7-B9'); 35 36 // Ekspor komposit B1-B7 dan B9 37 Export.image.toDrive({ 38 image: compositeB79, 39 description: 'Composite_B1_B7_B9_Export', 40 scale: 30, 41 region: ROI, 42 fileFormat: 'GeoTIFF', 43 maxPixels: 1e8 44 }); 45 </pre>

Figure 3. Script pre-processing

The results of the pre-processing stage are shown in Figure 4, which displays the output of Landsat imagery after undergoing radiometric correction, band compositing, and clipping and cropping according to the study area. This pre-processing provides an overview of the condition of Landsat image data, which is ready for further analysis related to land cover changes.

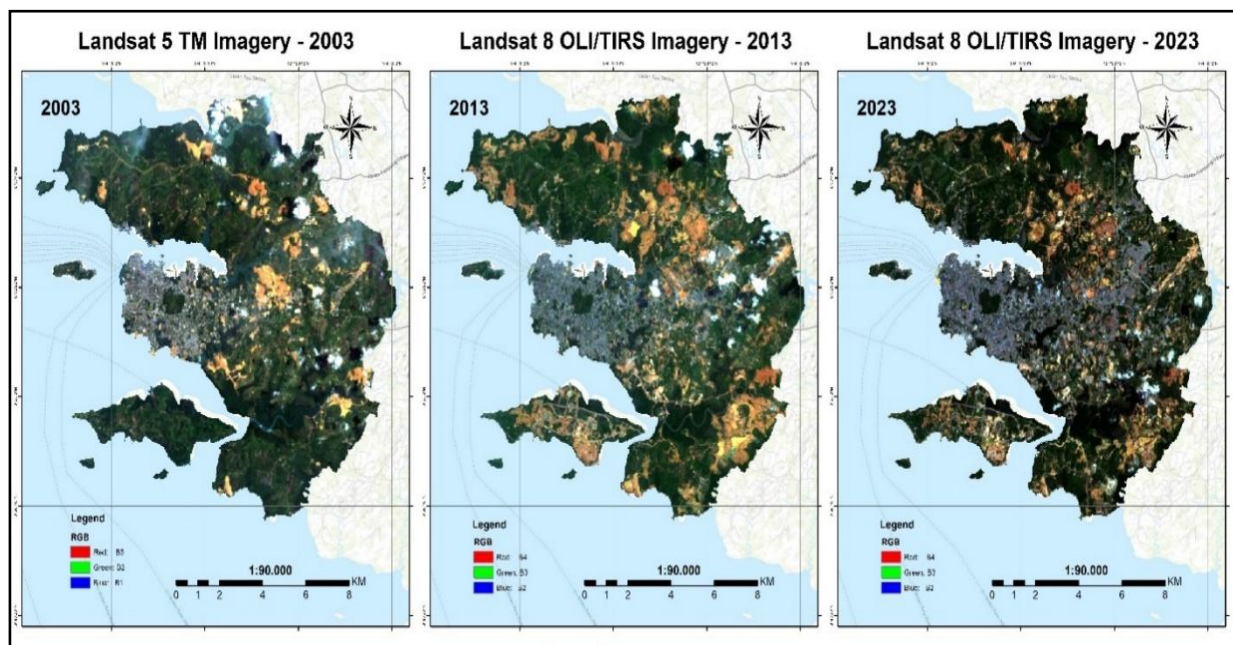
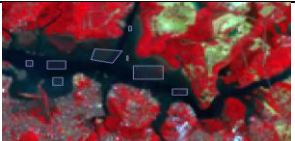

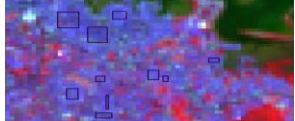
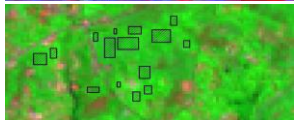


Figure 4. Landsat imagery map

3.2 Land Cover Classification

The land cover classification process is carried out by determining the training sample area. The more samples used, the better the accuracy of the classification results [32]. Sample determination is based on land cover categories, which include Water Bodies, Built-up Areas, Bare Land, and Vegetation. Class grouping is carried out through Landsat image interpretation based on a combination of bands, taking into account visual characteristics such as texture, colour, and pattern.

Table 3. Land cover training sample area

Land Cover	Training Sample Area	Band Combination		Description
		L 5 TM	L 8 OLI	
Water Body		432	543	The water body is a combination of waters in the form of rivers, lakes, and reservoirs, based on a combination of 543, which is pitch black with a smooth texture.
Bare Land		742	753	Bare land is dry land that lacks elements of development or vegetation growth. Based on the combination of 753, it appears to be a light brown.
Built-up Area		245	536	Settlements are areas of built-up area that are close together and dense, based on the combination of 536 in blue.
Vegetation		742	753	Vegetation is green land covered with forests, bushes, or gardens. In the combination of band 753, the vegetation area appears bright green.

The following process is to perform a Maximum Likelihood Classification (MLC) analysis based on the training category of land cover samples in Landsat images in 2003, 2013 and 2023, and a smoothing process is carried out on the classification results; the classification smoothing process aims to minimize the error value in the pixels being analyzed. The classification results on Landsat images in 2003, 2013, and 2023 are presented in Figure 5

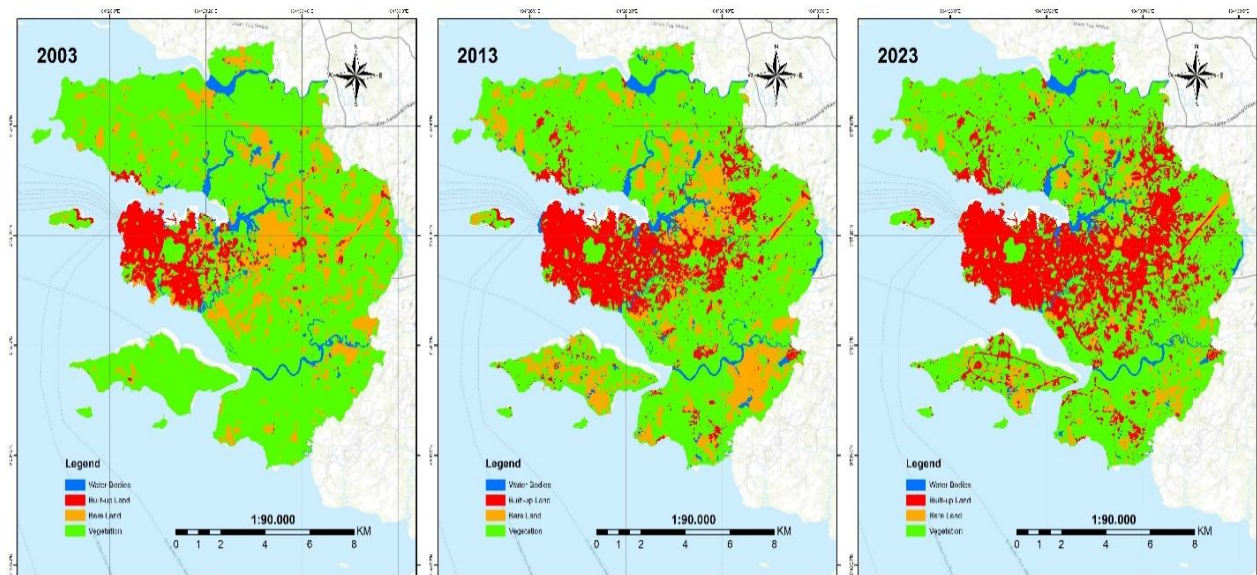


Figure 5: Classification results of landsat imagery for 2003, 2013, and 2023

Based on the land cover classifications conducted in 2003, 2013, and 2023, the results obtained were that in 2003, the area of water bodies was recorded at 4.54 km² or approximately 3.02% of the total area. This area increased in 2013 to 4.88 km² (3.24%) but decreased again in 2023 to 4.15 km² (2.76%). The built-up area shows a significant increasing trend, namely from 11.34 km² (7.54%) in 2003 to 25.34 km² (16.85%) in 2013, and continues to increase to reach 38.49 km² (25.59%) in 2023. Meanwhile, the area of bare land experienced a slight increase from 23.75 km² (15.79%) in 2003 to 25.21 km² (16.76%) in 2013, but then decreased drastically to 11.02 km² (7.33%) in 2023. Meanwhile, the most significant land cover type, vegetation cover, experienced a decrease in the area from 110.75 km² (73.64%) in 2003 to 94.96 km² (63.14%) in 2013. Although the vegetation area increased again to 96.73 km² (64.32%) in 2023, the overall trend remained downward compared to the initial year of observation.

Table 4. Land cover change in 2003, 2013, and 2023

Land Cover	2003		2013		2023	
	Area (Km2)	Percentage (%)	Area (Km2)	Percentage (%)	Area (Km2)	Percentage (%)
Water Body	4.54	3	4.88	3	4.15	3
Built-up Area	11.34	8	25.34	17	38.49	26
Bare Land	23.75	16	25.21	17	11.02	7
Vegetation	110.75	74	94.96	63	96.73	64
Total	150.38	100	150.38	100	150.38	100

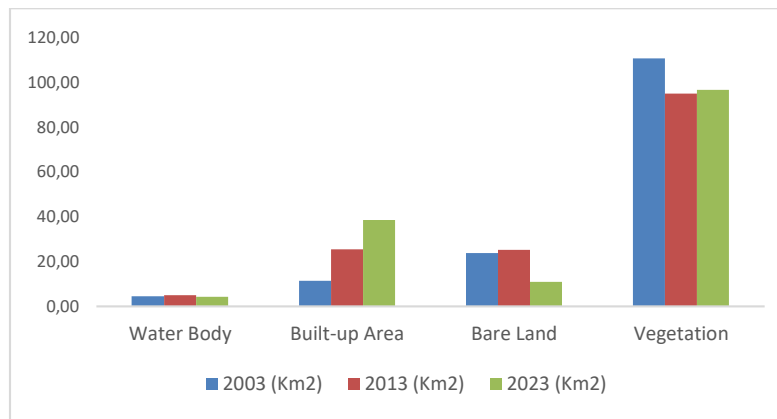


Figure 6. Land Cover Change Graph for 2003, 2013, and 2023

3.3 Land Cover Change

Land cover changes observed from 2003 to 2013, 2013 to 2023, and overall from 2003 to 2023 reveal the dynamics of space use that reflect changes in regional conditions. The built-up area experienced the most significant increase [33], specifically 14.01 km² between 2003 and 2013 and 13.14 km² between 2013 and 2023, resulting in a total rise of 27.15 km² over the last two decades. In contrast, vegetation cover experienced a sharp decline of 15.79 km² in the first period, followed by a slight increase of 1.77 km² in the following decade [34]. Overall, vegetation coverage declined by 14.02 km² from 2003 to 2023. On bare land, there was an increase of 1.45 km² from 2003 to 2013, followed by a drastic decrease of 14.19 km² from 2013 to 2023, resulting in a total decline of 12.74 km² from 2003 to 2023. This indicates that bare land emerged due to a decrease in Vegetation and was subsequently converted into a built-up area. Meanwhile, water bodies experienced small fluctuations, with an increase of 0.33 km² in the first decade, followed by a decrease of 0.72 km² in the subsequent decade. In total, there was a decline in water bodies of 0.39 km² over two decades, which, although small in quantitative terms, still reflects physical changes in the water elements in the area.

Land cover changes in Tanjungpinang City exhibit a pattern consistent with the findings of studies in other coastal cities in Indonesia. For example, in Jayapura City, there has been a decrease in vegetation cover of up to 67.28% [35], which reflects the impact of development on the environment. Although the scale of change differs, both in Tanjungpinang and Jayapura, a similar trend is observed, namely the reduction of green areas due to increased development of built-up areas. This development pressure on the environment is not only a local issue but also a widespread problem that affects various coastal areas. This finding is also supported by the study of [36], which shows that coastal development in Java Island has caused massive conversion of natural Vegetation, including mangroves and wetlands, into built-up areas and supporting infrastructure. Thus, land cover changes in Tanjungpinang are part of a broader phenomenon related to development pressure in coastal areas in Indonesia.

Table 5. Land cover change in 2003, 2013, and 2023

Land Cover	Year 2003 (Km2)	Year 2013 (Km2)	Year 2023 (Km2)	Difference 2003 & 2013 (Km2)	Difference 2013 & 2023 (Km2)	Difference 2003 & 2023 (Km2)
Water Body	4.54	4.88	4.15	0.33	-0.72	-0.39
Built-up Area	11.34	25.34	38.49	14.01	13.14	27.15
Bare Land	23.75	25.21	11.02	1.45	-14.19	-12.74
Vegetation	110.75	94.96	96.73	-15.79	1.77	-14.02

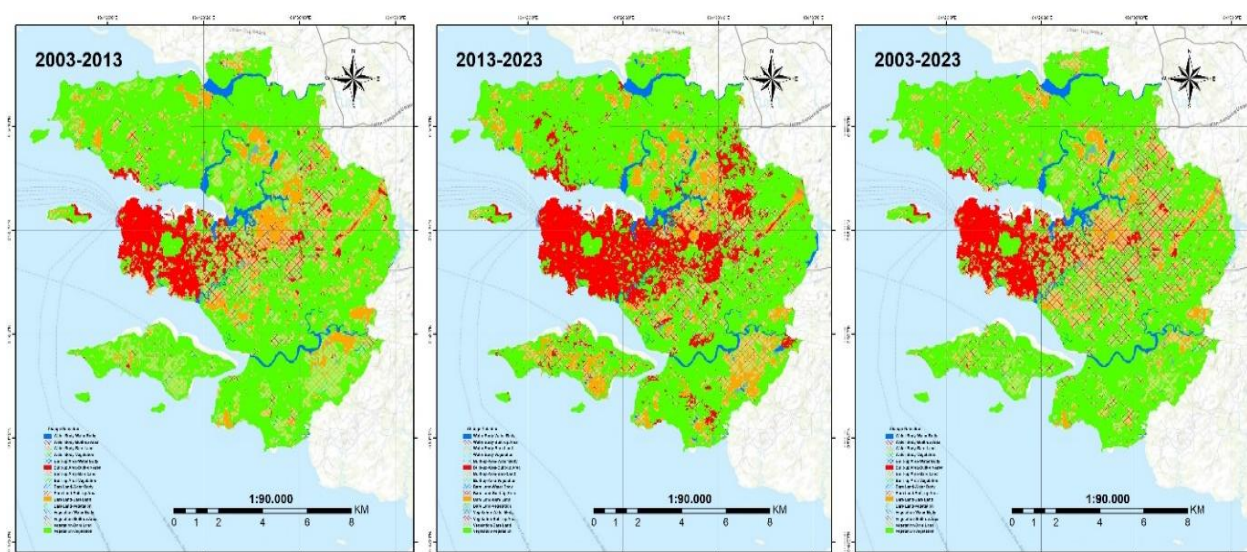


Figure 7. Land cover change map 2003-2013, 2013-2023 & 2003-2023

3.4 Land Cover Prediction

Land cover prediction in 2043 begins with a model accuracy test using data from 2003 and 2013 to predict conditions in 2023. The prediction results are validated against actual 2023 data using the Kappa Accuracy method as the basis for model feasibility. Once deemed feasible, the prediction is continued until 2043 through two iterations, each representing 10 years.

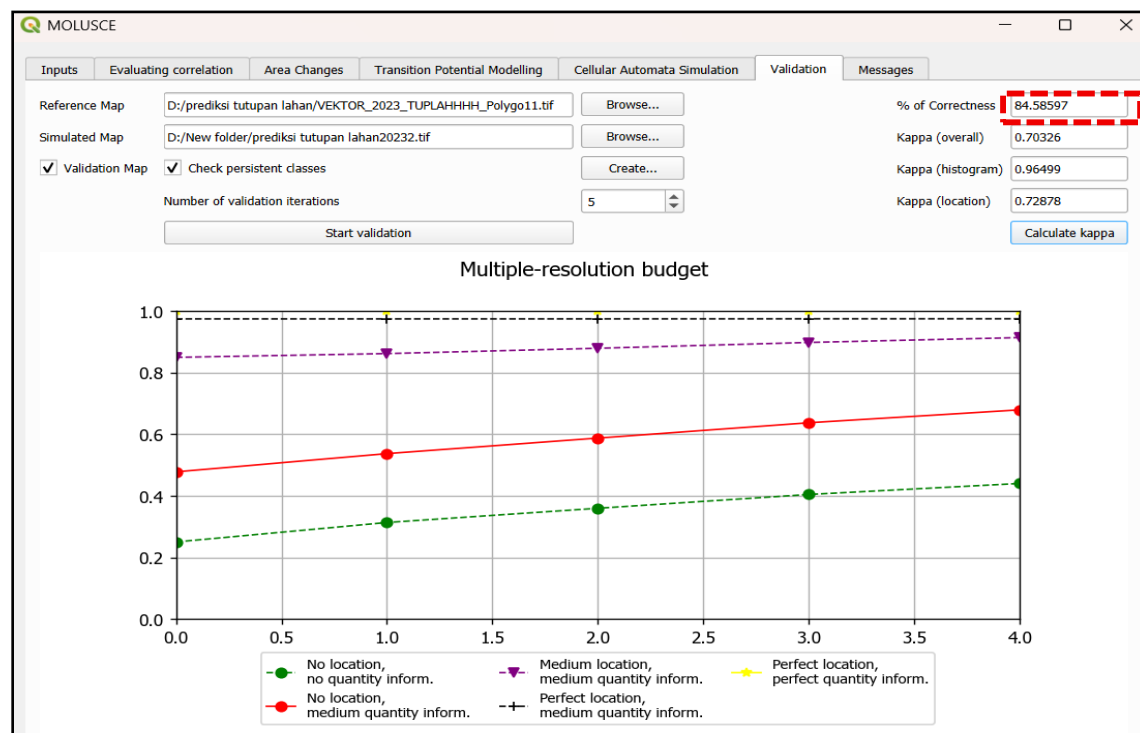


Figure 8. Modelling Accuracy

The results of the 2023 land cover prediction validation, as shown in Figure 8, indicate an accuracy level of 84.58%, which falls within the "Very Good" category according to the Kappa value interpretation [29]. This suggests that the agreement between the prediction results and the actual data is very high. Thus, the predictive model used is considered reliable and can be trusted to project future changes in land cover [37]. This high level of accuracy is a strong basis for continuing predictions until 2043.

Table 6. Land cover change in 2003, 2013, and 2023

Lann Cover	Existing 2023 (Km2)	Prediction 2023 (Km2)
Water Body	4.15	5.14
Built-up Area	38.49	35.42
Bare Land	11.02	13.25
Vegetation	96.73	96.57
Total	150.38	150.38
Kappa Accuracy	0.845859	
Kappa Accuracy (%)	84.58	

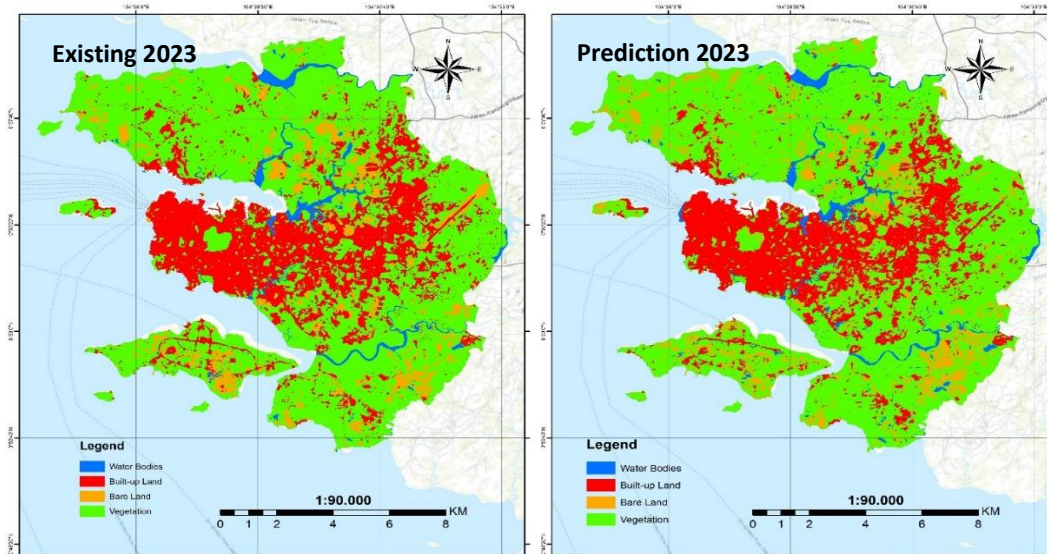


Figure 9. Maps of existing and predicted land cover

Comparison between predicted results and actual land cover conditions in 2023. The Built-up Area category experienced a difference of 3.07 km², where the expected area was slightly lower than the exact area. For the Bare Land category, there was a difference of 2.23 km², with the predicted area being higher than the existing data. Meanwhile, Water Body showed a difference of 0.99 km², while Vegetation had the most minor difference, at 0.16 km², between the predicted results and actual conditions.

The differences in area within each land cover class indicate that there is variation between the model's prediction results and reality in the field. However, overall, the Kappa value of 84.58% obtained from the validation process indicates that the model has excellent performance in simulating spatial patterns of land cover change [29]. This value provides a strong basis for continuing the land cover prediction process into the following years.

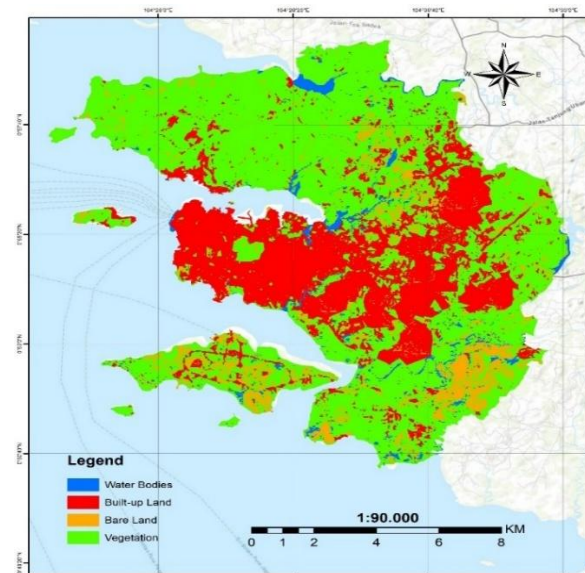


Figure 10. Land Cover Prediction Map for 2043

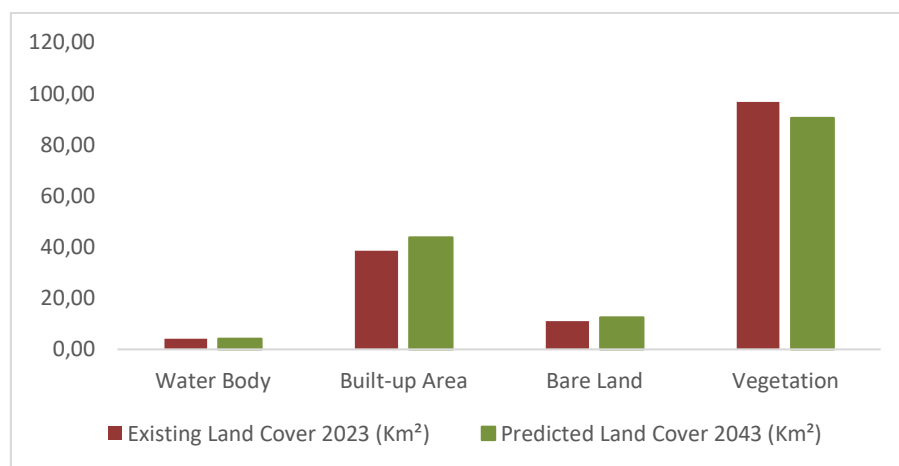


Figure 11. Land cover change graph from 2023 to 2043

Land cover predictions for 2043 show significant changes in several land cover categories compared to existing conditions in 2023. The Built-up Area category increased by 5.12 km², from 38.49 km² to 43.61 km². This change signifies a substantial expansion of built-up areas, reflecting the trend of regional development toward urbanization and increased development activities, including settlements, public facilities, and infrastructure. In contrast, the Vegetation category decreased by 6.33 km², from 96.73 km² to 90.40 km². This decrease indicates the conversion of vegetative land to other uses, which is most likely related to the increasing need for land for development.

The Bare Land category showed an increase of 1.34 km², from 11.02 km² to 12.36 km². This could indicate the process of opening new land that has not been optimally utilized, which is likely related to development activities or the conversion of vegetative land [6]. Meanwhile, the Water Body cover experienced little change, decreasing by 0.14 km², from 4.15 km² to 4.01 km², reflecting the relative stability of the water area over the last 20 years. Overall, the results of this

prediction provide an overview of the direction of land use changes, which are increasingly directed towards physical development, especially the expansion of built-up areas, that directly or indirectly affect the decline in vegetation area [28].

The findings of this study provide an important contribution to supporting spatial planning policies, especially in coastal areas such as Tanjungpinang City. Information on land cover changes that have occurred and predictions for the period until 2043 can be used by local governments as a basis for compiling a more targeted Regional Transport and Regional Water (RTRW). This data can help identify areas experiencing high development pressure so that stricter environmental control or protection is needed. In addition, the results of this prediction are also helpful as a tool to anticipate long-term environmental impacts, such as reduced green open space and increased flood risk due to uncontrolled urbanization [38].

In terms of education, the results of this study can serve as a concrete example to illustrate the impact of development on the environment. This material is relevant for learning related to geography, environment, and regional and city planning. Visualization and analysis of land cover change data over time facilitate an understanding of the importance of maintaining a balance between development and environmental sustainability [39]. In addition, the predictive approach employed in this study also introduces the use of geospatial technology as an analytical tool that plays a crucial role in sustainable development planning.

4. Conclusion

Land cover changes in Tanjungpinang City from 2003 to 2023 exhibit significant spatial shifts. Built-up land cover experienced the sharpest increase, from 11.34 km² (7.54%) in 2003 to 38.49 km² (25.59%) in 2023. This increase reflects the rapid process of urbanization and infrastructure development in response to population growth and economic activity. In contrast, vegetation cover decreased from 110.75 km² (73.64%) to 96.73 km² (64.32%), indicating pressure on the natural environment due to land conversion. Open land, which had increased to 25.21 km² in 2013, decreased again to 11.02 km² in 2023 due to its conversion into built-up areas. Waterbody cover is relatively stable, but the fluctuations that occur remain relevant as indicators of changes in coastal ecosystems. Predictions up to 2043 show a consistent trend of change, where built-up land is estimated to increase to 43.61 km², Vegetation decreases to 90.40 km², open land increases slightly to 12.36 km², and water bodies decrease to 4.01 km². Validation of the predictive model using 2023 data yielded an accuracy value of 84.58% with a Kappa value that falls within the "very good" category. This demonstrates that the approach employed (a combination of logistic regression and Cellular Automata) is effective in mapping land cover dynamics spatially and temporally.

Scientifically, this study contributes to the development of a land use change prediction model based on multi-temporal spatial data that can be replicated for other areas. In terms of application, the results of this study can be utilized by local governments and stakeholders as a scientific reference in the preparation and review of the Tanjungpinang City Spatial Plan (RTRW). This spatial information can also be used to identify areas with high development pressure, allowing for more focused land conversion control and area protection.

As a suggestion further research is suggested to integrate socio-economic dimensions and regional development policy directions as driving variables in the prediction model. In addition, the use of high-resolution satellite imagery and field survey data can improve the accuracy of the analysis and answer the need for more detailed spatial data in sustainable regional planning.

References

- [1] Afuye, G. A., Nduku, L., Kalumba, A. M., Santos, C. A. G., Orimoloye, I. R., Ojeh, V. N., Thamaga, K. H., & Sibandze, P. (2024). Global trend assessment of land use and land cover changes: A systematic approach to future research, development, and planning. *Journal of King Saud University - Science*.
- [2] Rustiadi, E., Pravitasari, A. E., Setiawan, Y., Mulya, S. P., Pribadi, D. O., & Tsutsumida, N. (2020). *Impact of continuous Jakarta megacity urban expansion on the formation of the Jakarta–Bandung conurbation over the rice farm regions*. *Cities*. Retrieved from
- [3] Sugianto, S., Deli, A., Miswar, E., Rusdi, M., & Irham, M. (2022). *The Effect of Land Use and Land Cover Changes on Flood Occurrence in the Teunom Watershed, Aceh Jaya*. *Land*, 11(8), 1271.
- [4] Afriyadi, A., Wulandari, A., Panjaitan, D. M., Saputra, E., Handoko, H., Isrania, I., Meilin, M., & Ernantonio, N. (2024). *Memahami dinamika ekonomi Tanjung Pinang: Potensi pengembangan dan rekomendasi kebijakan untuk kesejahteraan masyarakat*. *Jurnal Inovasi Ekonomi Syariah dan Akuntansi (JIESA)*, 1(4), 65–74.
- [5] Armayani, R. R., Lubis, H. K., & Sari, N. (2022). *Hubungan antara ekonomi dengan lingkungan hidup: Suatu kajian literatur*. *SINOMIKA Journal*, 1(2), 175.
- [6] Siswanto, S., Nuryanto, D. E., Ferdiansyah, M. R., Prastiwi, A. D., Dewi, O. C., Gamal, A., & Dimyati, M. (2023). *Spatio-temporal characteristics of the urban heat island in the Jakarta metropolitan area*. *Remote Sensing Applications: Society and Environment*, 32, 101062.
- [7] Hasyim, A. W., Sukojo, B. M., Anggraini, I. A., Fatahillah, E. R., & Isdianto, A. (2025). *Urban heat island effect and sustainable planning: Analysis of land surface temperature and Vegetation in Malang City*. *International Journal of Sustainable Development and Planning*, 20(2), 683–697.
- [8] Dinas Lingkungan Hidup dan Kehutanan Provinsi Kepulauan Riau. (2021). *Rencana Strategis Dinas Lingkungan Hidup dan Kehutanan Provinsi Kepulauan Riau Tahun 2021–2026*. Dinas Lingkungan Hidup dan Kehutanan Provinsi Kepulauan Riau.
- [9] Jawarneh, R. N., Abulibdeh, A., Hashem, N., Awawdeh, M., Al-Awadhi, T., Abdullah, M. M., & El Kenawy, A. M. (2024). *Assessing and predicting land cover dynamics for environmental sustainability in Jordan's arid ecosystems using the CA-Markov model*. *Remote Sensing Applications: Society and Environment*, 33, 101262.
- [10] Dewi, C. C., Pravitasari, A. E., & Pribadi, D. O. (2023). *Arahan pengembangan kawasan permukiman di Kota Tanjungpinang, Provinsi Kepulauan Riau*. *Jurnal Ilmu Tanah dan Lingkungan (J. Il. Tan. Lingk.)*, 25(1), 7–18.
- [11] Ramadhan, G. F., & Hidayati, I. N. (2022). *Prediction and simulation of land use and land cover changes using open source QGIS: A case study of Purwokerto, Central Java, Indonesia*. *Indonesian Journal of Geography*, 54(2), 172–180.
- [12] Nguyen, A., Kovyazin, V., & Pham, C. (2025). *Application of remote sensing and GIS in monitoring forest cover changes in Vietnam based on natural zoning*. *Land*, 14(5), 1037.
- [13] Allan, A., Soltani, A., Abdi, M. H., & Zarei, M. (2022). *Driving forces behind land use and land cover change: A systematic and bibliometric review*. *Land*, 11(8), 1222.
- [14] Lin, J., Li, X., Wen, Y., & He, P. (2022). *Modelling urban land-use changes using a landscape-driven patch-based cellular automaton (LP-CA)*. *Cities*, 129, 103906.
- [15] Laksmana, M. B., Zakaria, A., Novianti, T. C., & Armijon. (2024). *Analisis prediksi perubahan tutupan lahan tahun 2033 menggunakan metode Cellular Automata dan Logistic Regression*. *Journal of Plano Studies*, 1(2), Desember. ISSN Online: 3047-2857.
- [16] Badan Pusat Statistik Kota Tanjungpinang. (2024). *Kecamatan Tanjungpinang Kota Dalam Angka 2024 / Tanjungpinang Kota Subdistrict in Figures 2024* (Vol. 21, Katalog: 1102001.2172010). BPS-Statistics Tanjungpinang Municipality.

-
- [17] Putra, R. D., Napitupulu, H. S., Nugraha, A. H., Suhana, M. P., Ritonga, A. R., & Sari, T. E. Y. (2022). *Pemetaan luasan hutan mangrove dengan menggunakan citra satelit di Pulau Mapur, Provinsi Kepulauan Riau. Jurnal Kelautan Tropis*, 25(1), 20–30.
 - [18] Vollrath, A., Mullissa, A., & Reiche, J. (2020). *Angular-based radiometric slope correction for Sentinel-1 on Google Earth Engine. Remote Sensing*, 12(11), 1867.
 - [19] Qiu, S., Zhu, Z., Olofsson, P., Woodcock, C. E., & Jin, S. (2021). *Evaluation of Landsat image compositing algorithms. Remote Sensing of Environment*, 256, 112307.
 - [20] Arinta, S. P. (2015). *Penggunaan citra satelit multi-temporal untuk kajian perubahan pola sungai dan lahan di sekitar aliran sungai pasca erupsi gunung api (Studi kasus: Sub DAS Konto)* (Tugas Akhir, Institut Teknologi Sepuluh Nopember). Jurusan Teknik Geomatika, Fakultas Teknik Sipil dan Perencanaan, ITS Surabaya.
 - [21] Egorov, A. V., Hansen, M. C., Roy, D. P., Kommareddy, A., & Potapov, P. V. (2015). *Image interpretation-guided supervised classification using nested segmentation. Remote Sensing of Environment*, 165, 135–147.
 - [22] Septiani, R., Citra, I. P. A., & Nugraha, A. S. A. (2019). Perbandingan metode supervised classification dan unsupervised classification terhadap penutup lahan di Kabupaten Buleleng. *Jurnal Geografi*, 16(2).
 - [23] Lu, D., Mausel, P., Batistella, M., & Moran, E. (2004). *Comparison of land-cover classification methods in the Brazilian Amazon Basin. International Journal of Remote Sensing*, 25(21), 5403–5417.
 - [24] Li, H., Wang, C., Zhong, C., Zhang, Z., & Liu, Q. (2017). *Mapping typical urban LULC from Landsat imagery without training samples or self-defined parameters. Remote Sensing*, 9(7), 700.
 - [25] García-Rodríguez, D., Pérez-Hoyos, A., Martínez, B., Catret Ruber, P., Samper-Zapater, J. J., López-Baeza, E., & Martínez Durá, J. J. (2025). *Comparative analysis of different algorithms for VAS station land cover classification with limited training points. International Journal of Applied Earth Observation and Geoinformation*, 139, 104537.
 - [26] Febianti, V., Sasmito, B., & Bashit, N. (2022). Pemodelan perubahan tutupan lahan berbasis penginderaan jauh (Studi kasus: Kota Semarang). *Jurnal Geodesi Undip*, Oktober, Departemen Teknik Geodesi, Fakultas Teknik, Universitas Diponegoro.
 - [27] Tiede, D. (2014). *A new geospatial overlay method for the analysis and visualization of spatial change patterns using object-oriented data modelling concepts. Cartography and Geographic Information Science*, 41(3), 227–234.
 - [28] Hapsary, M. S. A., Subiyanto, S., & Firdaus, H. S. (2021). Analisis Prediksi Perubahan Penggunaan Lahan dengan Pendekatan Artificial Neural Network dan Regresi Logistik di Kota Balikpapan. *Jurnal Geodesi Undip*, April 2021. Departemen Teknik Geodesi, Fakultas Teknik, Universitas Diponegoro.
 - [29] Fardani, I., Mohmed, F. A. J., & Chofyan, I. (2020). *Pemanfaatan Prediksi Tutupan Lahan Berbasis Cellular Automata-Markov dalam Evaluasi Rencana Tata Ruang. MKG*, 21(2), 157–169. P-ISSN: 0216-8138 | E-ISSN: 2580-0183.
 - [30] Juniyanti, L., Prasetyo, L. B., Aprianto, D. P., Purnomo, H., & Kartodihardjo, H. (2020). *Perubahan penggunaan dan tutupan lahan, serta faktor penyebabnya di Pulau Bengkalis, Provinsi Riau (periode 1990–2019). Journal of Natural Resources and Environmental Management*, 10(3), 419–435. E-ISSN: 2460-5824.
 - [31] Hariyati, E. (2024). *Prediksi perubahan tutupan/penggunaan lahan tahun 2036 di Kecamatan Kotabumi Utara menggunakan model Cellular Automata* (Skripsi Sarjana). Fakultas Keguruan dan Ilmu Pendidikan, Universitas Lampung, Bandar Lampung.
 - [32] Waśniewski, A., Hościło, A., & Aune-Lundberg, L. (2023). The impact of the selection of reference samples and DEM on the accuracy of land cover classification based on Sentinel-2 data. *Remote Sensing Applications: Society and Environment*, 32, 101035.
-

-
- [33] Demessie, S. F., Dile, Y. T., Bedadi, B., Tarkegn, T. G., Bayabil, H. K., & Sintayehu, D. W. (2024). *Assessing and projecting land use land cover changes using machine learning models in the Guder watershed, Ethiopia*. *Environmental Challenges*, 9, 101074.
- [34] Bodner, G. S., & Robles, M. D. (2017). *Enduring a decade of drought: Patterns and drivers of vegetation change in a semi-arid grassland*. *Journal of Arid Environments*, 136, 1–14.
- [35] Pamungkas, G. B., & Andriani, V. (2023). Contribution of land use change and land cover to climate change coastal areas and their impacts: Evidence in Jayapura City, Papua Province, Indonesia. *Jurnal Wilayah dan Lingkungan*, 11(1), 36–46.
- [36] Nofirman, N., Harahap, M. A. K., & Andiani, P. (2023). Studi geomorfologi dan perubahan lanskap dalam konteks perubahan lingkungan di Pulau Jawa. *Jurnal Geosains West*
- [37] Selmy, S. A. H., Kucher, D. E., Mozgeris, G., Moursy, A. R. A., Jimenez-Ballesta, R., Kucher, O. D., Fadl, M. E., & Mustafa, A. A. (2023). Detecting, analyzing, and predicting land use/land cover (LULC) changes in arid regions using Landsat images, CA-Markov hybrid model, and GIS techniques. *Remote Sensing*, 15(23), 5522.
- [38] Putra, R. A., Dewi, A. R., & Prasetyo, L. B. (2022). Analisis perubahan tutupan lahan untuk mendukung perencanaan tata ruang wilayah pesisir berbasis geospasial. *Jurnal Perencanaan Wilayah dan Kota*, 19(1), 55–66.
- [39] Sofyan, A., & Ridwan, M. (2023). Integrasi pembelajaran geospasial dalam kurikulum sekolah menengah: Studi kasus perubahan lahan di Kota Padang. *Jurnal Pendidikan Geografi*, 11(2), 93–107.